



ELSEVIER

Available online at [www.sciencedirect.com](http://www.sciencedirect.com)

SCIENCE @ DIRECT®

Nuclear Instruments and Methods in Physics Research B 230 (2005) 172–177

**NIM B**  
Beam Interactions  
with Materials & Atoms

[www.elsevier.com/locate/nimb](http://www.elsevier.com/locate/nimb)

# Interatomic potentials from rainbow scattering of keV noble gas atoms under axial surface channeling

A. Schüller<sup>a</sup>, S. Wethekam<sup>a</sup>, A. Mertens<sup>a</sup>, K. Maass<sup>a</sup>,  
H. Winter<sup>a,\*</sup>, K. Gärtner<sup>b</sup>

<sup>a</sup> *Institut für Physik der Humboldt-Universität zu Berlin, Physik der Grenzflächen und dünnen Schichten (PGD),  
Newtonstrasse 15, D-12489 Berlin-Adlershof, Germany*

<sup>b</sup> *Physikalisch-Astronomische, Friedrich-Schiller-Universität, Max-Wien-Platz 1, D-07743 Jena, Germany*

Available online 21 January 2005

## Abstract

For grazing scattering of keV Ne and Ar atoms from a Ag(111) and a Cu(111) surface under axial surface channeling conditions we observe well defined peaks in the angular distributions for scattered projectiles. These peaks can be attributed to “rainbow-scattering” and are closely related to the geometry of potential energy surfaces which can be approximated by the superposition of continuum potentials along strings of atoms in the surface plane. The dependence of rainbow angles on the scattering geometry provides stringent tests on the scattering potentials. From classical trajectory calculations based on universal (ZBL), adjusted Moliere (O’Connor and Biersack), and individual interatomic potentials we obtain corresponding rainbow angles for comparison with the experimental data. We find good overall agreement with the experiments for a description of trajectories based on adjusted Moliere and individual potentials, whereas the agreement is poorer for potentials with ZBL screening.

© 2004 Elsevier B.V. All rights reserved.

PACS: 79.20.Rf

Keywords: Ion surface scattering; Atomic potential; Metal surface

## 1. Introduction

In atomic collisions interaction potentials play an essential role, since those potentials are directly

related to the outcome of binary encounters. In a classical description, interatomic potentials determine the trajectories of the collision partners and can be used to derive deflection functions (dependence of scattering angle on impact parameter) and differential cross-sections [1]. Also the distance of closest approach of colliding atoms or ions can be obtained from the interaction potentials which

\* Corresponding author. Tel.: +49 30 2093 7891; fax: +49 30 2093 7899.

E-mail address: [winter@physik.hu-berlin.de](mailto:winter@physik.hu-berlin.de) (H. Winter).

might be important to identify interaction mechanisms during the encounter. In a quantal approach, interaction potentials directly enter the scattering amplitudes for the calculations of cross-sections [2].

For collisions of fast atoms and ions with typical energies in the keV range, the interatomic potentials are crucial for calculations of projectile trajectories from classical mechanics in order to model a variety of processes as stopping phenomena, electronic excitations, charge transfer, or focusing effects. As a consequence, a wide body of work and literature is devoted to provide generalized expressions for those potentials [3]. Of particular interest are generalized descriptions of the potentials which are mostly based on the statistical Thomas–Fermi model for taking into account electronic screening effects in atoms. These screened Coulomb potentials are characterized by screening functions which are constructed by sums of exponential functions with a screening length  $a_s$  being the reference for the length scale (atomic units are used throughout this paper)

$$V(r) = \frac{Z_1 Z_2}{r} \sum_i a_i \exp(-b_i r/a_s) \quad (1)$$

with  $Z_1$  and  $Z_2$  being the nuclear charge of the atoms and  $a_i$  and  $b_i$  are parameters of the screening functions. In the approach by Moliere [4] one has  $a_i = \{0.35, 0.55, 0.1\}$  and  $b_i = \{0.3, 1.2, 6\}$  with the Firsov screening length  $a_s = a_F = 0.8854$  a.u.  $(Z_1^{1/2} + Z_2^{1/2})^{-2/3}$ . For the “universal potential” Ziegler, Biersack and Littmark (ZBL) [3] proposed  $a_i = \{0.1818, 0.5099, 0.2802, 0.02817\}$  and  $b_i = \{3.2, 0.9423, 0.4028, 0.2016\}$  with the universal screening length  $a_s = a_u = 0.8854$  a.u.  $(Z_1^{0.23} + Z_2^{0.23})$ . O’Connor and Biersack suggested an improved description of the Moliere potential by a correction of the Firsov screening length according to  $a_s = a_{OCB} = [\alpha(Z_1^{1/2} + Z_2^{1/2}) + \beta]a_F$  with  $\alpha = 0.045$  and  $\beta = 0.54$  [5].

These generalized interatomic potentials are smooth functions with respect to the interatomic distance  $r$  and the atomic numbers  $Z_1$  and  $Z_2$  and do not take into account the electronic shell structure of the atoms. Such effects can be taken into account by considering an “individual poten-

tial” which is calculated numerically for each  $Z_1$ – $Z_2$ -combination. In our work we use a statistical model taking into account the electrostatic, kinetic and exchange contributions. The calculations are based on electron distributions of free atoms which are obtained from electron wave functions given by Clementi and Roetti [6] and are free from adjustable parameters. Details on the calculations of the individual potentials can be found in [7].

In this paper we report on studies of the scattering of fast Ne and Ar atoms from metal surfaces under a grazing angle of incidence. By making use of so called “rainbow” structures in the angular distributions for scattered projectiles present for scattering along a low index crystallographic direction in the surface plane (“axial surface channeling”), we explore the atomic interaction potentials at surfaces in the range from 1 eV to several 10 eV. It turns out that the angular positions of these “rainbows” depend strongly on the scattering potential [8] and can be used for stringent tests of interaction potentials at surfaces [9,10].

## 2. Experiment and simulation

In our experiments we have scattered neutral Ne and Ar atoms with energies ranging from 1 keV to 100 keV from Ag(111) and Cu(111) under a grazing angle of incidence  $0.5^\circ \leq \Phi_{in} \leq 2^\circ$  with an azimuthal setting along low index crystallographic directions in the surface plane (surface channeling conditions). The azimuthal orientation of the target surface relative to the incident beam was obtained via a rotary feed through of a precision manipulator. Neutral projectiles are used here, in order to avoid effects of the image charge present for ionized projectiles. In experiments with ions we found angular shifts up to several degrees, consistent with effective image charge interaction energies in the eV domain [11]. The neutral projectiles were produced via resonant charge transfer in a target operated with Ne or Ar gas in the beam line of the accelerator. The projectile beam is collimated by sets of vertical and horizontal slits of 0.2 mm width to a divergence of about 0.1 mrad. The target surface is prepared by cycles of sputtering with 25 keV  $Ar^+$  ions under a grazing angle of

incidence of typically  $2^\circ$  and subsequent annealing to temperatures of about  $500^\circ\text{C}$ . The scattered projectiles are recorded by a commercially available position-sensitive channelplate detector [12] located 66 cm behind the target. In order to avoid dead time effects in the counting of events, the primary beam was reduced to a current which resulted in maximum count rates at the detector of less than  $10^4$  counts per second. The resulting current under these conditions amounts to typically some fA so that radiation damage of the surface by the impinging atoms is negligible.

For comparison with data, the scattering of the Ne and Ar atoms is simulated by calculations of classical trajectories. Because of the small angle between the incident beam and a low index crystallographic direction ( $x$ -axis) in the surface plane ( $x$ ,  $y$ -plane), projectile atoms move with about constant velocity in the low index direction. The motion in the ( $y$ ,  $z$ )-plane is determined by the sum of all interaction potentials between projectile and target atoms which is for channeling conditions well approximated by continuum potentials derived from an averaging of pair potentials over atomic strings [13]. In passing we note that trajectories calculated in molecular dynamics computer simulations are very close to those obtained using the continuum approach [14]. For motion of atoms in the ( $y$ ,  $z$ )-plane only a few neighbouring strings of the topmost atomic layer and of the layer beneath the surface have to be taken into account. The trajectories in the ( $y$ ,  $z$ )-plane are derived from two-dimensional equations of motion with the initial velocities  $v_y = 0$  and  $v_z = v_0 \sin \Phi_{\text{in}}$  (initial transverse energy  $E_z = E_0 \sin^2 \Phi_{\text{in}}$ ).

### 3. Results and discussion

In Fig. 1 we show 2D-plots of some typical angular distributions obtained for scattering of 2 keV, 4 keV, 8 keV and 18 keV Ar atoms from a Ag(111) surface under  $\Phi_{\text{in}} = 1.8^\circ$  along a  $\langle 110 \rangle$  direction in the surface ( $E_z \approx 2$  eV, 4 eV, 8 eV, 18 eV, respectively). The data reveal clearly prominent peaks under these scattering conditions which can be ascribed to rainbow scattering caused by the sinusoidal corrugation of the “effec-

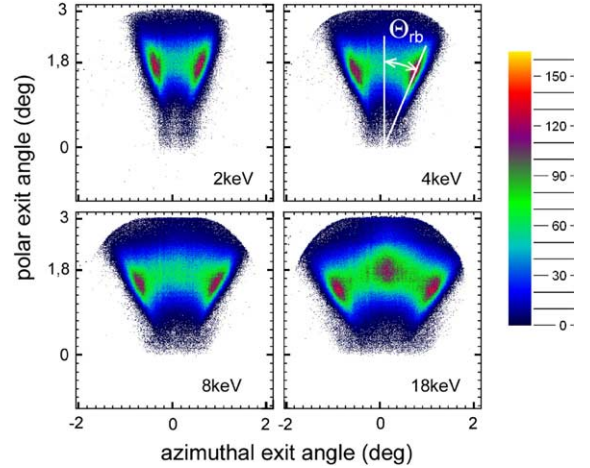


Fig. 1. Two-dimensional plots of angular distributions recorded by means of position sensitive channelplate detector for scattering of 2 keV, 4 keV, 8 keV and 18 keV Ar atoms from Ag(111) under  $\Phi_{\text{in}} = 1.8^\circ$ .

tive potential” in  $y$ -direction [9,10]. The opening angle between the two peaks amounts to twice of the corresponding rainbow angle  $\Theta_{\text{rb}}$  which can be precisely derived from defined angular distributions as shown in the figure. Note that projectiles with higher  $E_z$  probe equipotential planes of enhanced potential energy with an enhanced corrugation. Therefore we observe larger rainbow angles for higher  $E_z$ . The peak in the centre of the angular distribution shown in the lower right panel of Fig. 1 is attributed to a pronounced double scattering between two adjacent axial strings at sufficiently large  $E_z$ .

The rainbow angle  $\Theta_{\text{rb}}$  for Ar atoms scattered from Ag(111) over the whole range of  $E_z$  investigated is presented in Fig. 2. The data reveal the expected monotonic enhancement with increasing  $E_z$  which can be understood by the stronger corrugation of the “effective potential” for larger transverse energies. The observed rainbow angles are compared with results from the simulations using different approaches for the description of the interatomic potentials given in Section 1. The dashed curve in Fig. 2 is the result of the simulations using the ZBL potential. It can be seen that for  $E_z$  up to about 40 eV they underestimate the experimental data heavily, i.e. the potential used is clearly too repulsive. This discrepancy is partic-

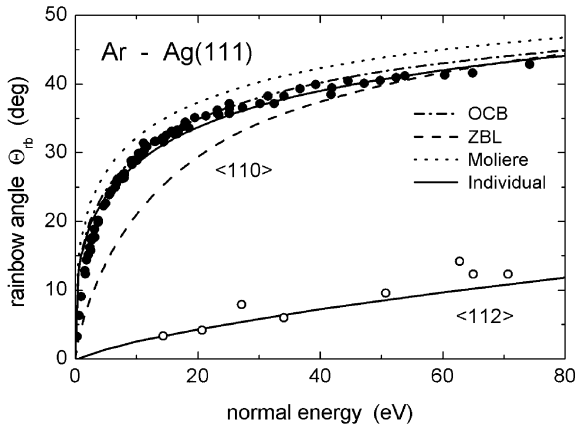


Fig. 2. Rainbow angle  $\Theta_{rb}$  as function of transverse energy  $E_z$  for scattering of Ar atoms from Ag(111) along  $\langle 110 \rangle$  (full circles) and  $\langle 112 \rangle$  (open circles). Curves represent results from simulations using OCB (dashed-dotted), ZBL (dashed), Moliere (dotted) and “individual” (solid) potentials.

ularly evident at small potential energies which are equivalent to large distances between the collision partners. The dashed-dotted curve represents calculations using the potential suggested by O’Connor and Biersack (OCB) which shows an overall better agreement with the experimental data as the pure Moliere or ZBL potential do. The solid curve shows the results obtained using the “individual” Ar–Ag potential calculated as described above. They agree very well with the experimental data over the complete range of transverse energies  $E_z$  studied here. As can be seen in Fig. 2, a reasonable agreement of the simulated result is obtained also for scattering along the  $\langle 112 \rangle$  azimuth. Since for this higher indexed axial direction distances between adjacent strings of atoms are smaller, the corrugation of the effective potential is smaller than for the  $\langle 110 \rangle$  direction. Therefore the rainbow angles are smaller in this case. We also recorded data for scattering of Ne atoms on Ag(111) (not shown) with similar results as for Ar projectiles.

Fig. 3 shows the interaction potential between an Ar and a Ag atom as a function of the distance and reveals a clearly too strong ZBL potential at larger distances compared to the “individual” potential. The OCB potential is fairly close to the “individual” potential over the complete range of relevant distances. This is the origin for the

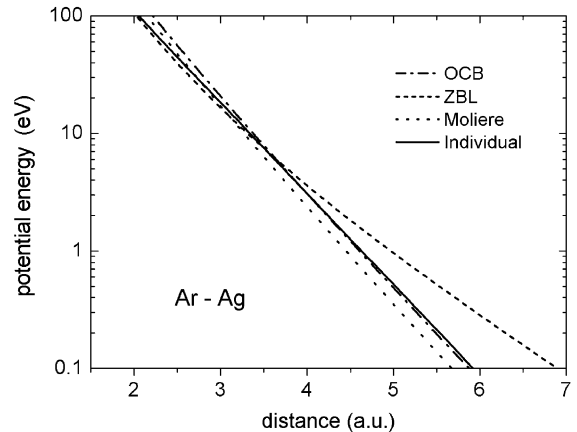


Fig. 3. Interatomic pair potentials for Ar–Ag as function of the distance between the atoms: OCB (dashed-dotted), ZBL (dashed), Moliere (dotted) and “individual” (solid) potential.

close agreement with the experimental data obtained by both potentials in the simulations of trajectories.

The data for the scattering of Ne atoms from a Cu(111) surface are given in Fig. 4. The rainbow angles show a similar dependence as found for scattering of Ar atoms from Ag(111). Calculations using the individual potential result also in this case in a good description of the experiments over the complete range of  $E_z$  studied here ( $E_z < 80$  eV)

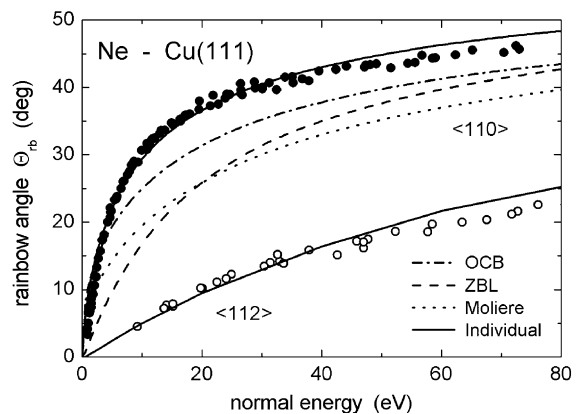


Fig. 4. Rainbow angle  $\Theta_{rb}$  as function of transverse energy  $E_z$  for scattering of Ne atoms from Cu(111) along  $\langle 110 \rangle$  (full circles) and  $\langle 112 \rangle$  (open circles). Curves represent results from simulations using OCB (dashed-dotted), ZBL (dashed), Moliere (dotted) and “individual” (solid) potentials.

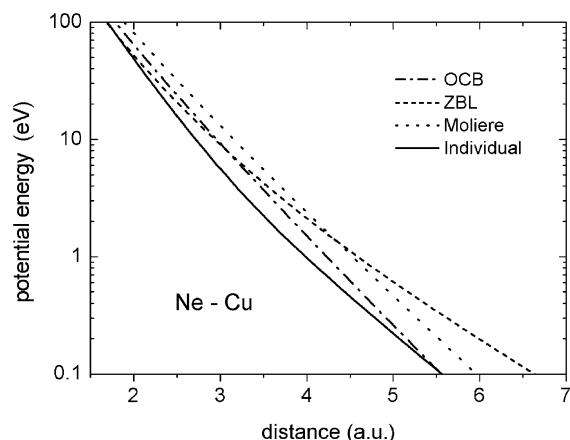


Fig. 5. Interatomic pair potentials for Ne–Cu as function of distance between the atoms: OCB (dashed-dotted), ZBL (dashed), Moliere (dotted) and “individual” (solid) potential.

for incidence along  $\langle 110 \rangle$  and  $\langle 112 \rangle$ . The other potentials used provide rainbow angles which underestimate the data.

Fig. 5 shows a plot of the corresponding interatomic potentials between a Ne and a Cu atom as function of the distance. In the semi-logarithmic plot it is evident that the ZBL potential is stronger than the other potentials for distances larger than about 3 a.u. Already in earlier studies evidence for this feature was obtained [9,10,15,16], however, a quantitative analysis of data was generally beyond the scope of past studies. Our analysis provides detailed information in this respect.

#### 4. Conclusions

In conclusion, we have presented an analysis of rainbow structures observed in the scattering of noble gas atoms from metal surfaces under axial surface channeling conditions. The well defined peaks in the angular distributions of scattered atoms allow us to analyze the data in terms of scattering potentials. It turns out that the rainbow angles are closely related to the geometrical structure of potential energy surfaces up to several 10 eV. This feature is the basis for detailed tests on established approaches for atomic pair potentials in an interval of distances from about 2–6 a.u. For the

specific cases studied here, i.e. Ne–Cu(111) and Ar–Ag(111), we find an overall good description of data by “individual” potentials, whereas Coulomb potentials with ZBL screening are generally too repulsive for larger distances. We also reveal that the application of a correction of the screening length in the Moliere potential as proposed by O’Connor and Biersack results in a better agreement with the experimental data.

Finally we note that our method allows us to perform detailed and general tests on interatomic potentials and on concepts for the description of screening phenomena by electron clouds of atoms. It bears also the potential to investigate the effect of the solid on the interaction potentials. In recent work with an Al surface, i.e. a metal with a higher density of conduction electrons than Cu and Ag, we found that the interaction potential has to be corrected with respect to the effect caused by embedding the atomic projectile into the electron gas of the seldge of the surface [17]. This contribution can amount to corrections for the interaction potentials of up to some eV and is repulsive for noble gas atoms but attractive for reactive atoms.

#### Acknowledgement

This work is supported by the Deutsche Forschungsgemeinschaft under contract Wi 1336.

#### References

- [1] E.W. McDaniel, J.B.A. Mitchell, M.E. Rudd, Atomic Collisions, Wiley, New York, 1993.
- [2] N.F. Mott, H.S.W. Massey, The Theory of Atomic Collisions, Oxford Press, Oxford, 1965.
- [3] J.F. Ziegler, J.P. Biersack, U. Littmark, The Stopping and Range of Ions in Solids, Vol. 1, Pergamon Press, New York, 1985.
- [4] G. Moliere, Z. Naturforsch. A 2 (1947) 133.
- [5] D.J. O’Connor, J.P. Biersack, Nucl. Instr. and Meth. B 15 (1986) 14.
- [6] E. Clementi, C. Roetti, At. Data Nucl. Data Tables 14 (1974) 177.
- [7] K. Gärtner, K. Hehl, Phys. Stat. Sol. (b) 94 (1979) 231.
- [8] A.W. Kley, T.C.M. Horn, Phys. Rep. 199 (1991) 191.

- [9] D.M. Danailov, R. Pfandzelter, T. Igel, H. Winter, K. Gärtner, *Appl. Surf. Sci.* 171 (2001) 113.
- [10] D. Danailov, K. Gärtner, A. Caro, *Nucl. Instr. and Meth. B* 153 (1999) 191.
- [11] H. Winter, *Phys. Rep.* 367 (2002) 387.
- [12] DLD40, Roentdek Handels GmbH, Kelkheim-Ruppersheim.
- [13] D. Gemmell, *Rev. Mod. Phys.* 46 (1974) 129.
- [14] D. Danailov, D.J. O'Connor, K.J. Snowdon, *Surf. Sci.* 347 (1996) 215.
- [15] R. Pfandzelter, F. Stölzle, H. Sakai, Y.H. Ohtsuki, *Nucl. Instr. and Meth. B* 83 (1993) 469.
- [16] B. Poelsema, L. Verhey, A. Boers, *Surf. Sci.* 64 (1977) 554.
- [17] A. Schüller, G. Adamov, S. Wethekam, K. Maass, A. Mertens, H. Winter, *Phys. Rev. A* 69 (2004) 050901 (R).